Published by :
http://www.ijert.org

International Journal of Engineering Research & Technology (IJERT)
ISSN: 2278-0181
Vol. 11 Issue 08, August-2022

Numerical Investigation on Flexural Behaviour of Inclined Stiffened Hollow Glulam Beam

Anu S. Das
Department of Civil Engineering
Government College of Engineering Kannur
Kannur, India

Rajesh K. N
Department of Civil Engineering
Government College of Engineering Kannur
Kannur, India

***Abstract*—Glulam is a manufactured wooden product emerging nowadays due to its numerous advantages and sustainability. The load-carrying capacity of stiffened hollow glulam beam depends on its aspect ratios, alignment of stiffeners, and inclination angle during bending. The present study conducted a numerical investigation using finite element models developed in ANSYS. For the aspect ratio with a constant width, the load-carrying capacity have been increased by about 180.72%. With a constant depth, the load carrying capacity increases to 32%. So, considering the aspect ratios with constant depth and constant width, the variation of depth has much significance. As the aspect ratio increases, the stiffness of the beam decreases. With a constant aspect ratio, the dimension greater than 150 mm × 150 mm has a much higher load-carrying capacity. About six different inclined stiffener pattern is adopted and obtained an optimum stiffener pattern, which has a much higher load-carrying capacity than the vertically stiffened hollow glulam beams. Then for the optimum pattern with inclined stiffeners, the inclination angle varied from 0° to 45°, and an optimum angle was obtained.**

Key Words: Glulam, Beam, Stiffeners, Bending, ANSYS

I. INTRODUCTION

Concrete structures, steel structures and composite structures are commonly seen all over the world. They have numerous advantages; however it is highly uneconomic and unsustainable, and it causes harmful effects on the environment during its construction and demolition. One remedial measure is using naturally available materials such as wood, bamboo, etc. Wooden veneers, flakes, or strands are bonded with moisture-resistant adhesives under certain heat and pressure for structural purposes. These glued wooden products are called Glulam (glued laminated engineered wood). Due to its ease of construction, glulam materials are commonly used nowadays. The naturally available stiffened product is bamboo, which has relatively high stiffness and stability on lateral loading. Inspired by bamboo, a newly engineered wood product that is hollow and has intermediate stiffeners are emerging. Generally, wooden products used in construction for structural purposes are solid. However, hollow timber products have also emerged in the last few decades due to its ductile property than the solid members. Glulam is created as a strong, long, and structural member, even in curved shapes.

Issa, Camille A., and Ziad Kmeid. [8] shows the generation of glulam beams. With the advancement in the wooden beam, additional reinforcement such as steel plates and CFRP are introduced between the timber. Then this product is glued and pressed. The result shows that the reinforced glulam beam provides a ductile failure and excessive deflection before failure. Zhang, Xiaofeng, Jing Luo, Lisheng Luo, Youfu Sun, and Zheng Li. [13] discuss the solid, hollow, and bamboo-like stiffened glulam beams and its bending behaviour. The result shows the most considerable elastic stiffness and load-carrying capacity for solid. However, a notable difference in these values is seen in hollow and bamboo-like stiffened glulam beams. Also, bamboo-like stiffened glulam beams have much higher ductile properties than solid and hollow glulam beams. It is due to the introduction of stiffeners to the beam. The thickness of the bottom plate, web plate, and spacing of stiffeners in bamboo-like stiffened glulam beams have a higher load-carrying capacity and elastic stiffness.

Fossetti, Marinella, et al. [7] shows that the glulam beam reinforced with FRP cords has a higher strength. The installation of the reinforcement induces compressive failure of the upper layer after cracking the beam, allowing a limited strength recovery. Also, basalt-reinforced glulam beams have better strength and ductility. Ferrier, E., P. Labossière, and K. W. Neale. [6] were created a hybrid beam with ultra-high-performance concrete, glued laminated wood, and FRP. The high young's modulus of the UHPC planks leads to the increased bending stiffeners. Also, an improvement in the ultimate capacity is seen due to the addition of lower concrete plank reinforced with steel or FRP rebars. So, the depth of the beam can be reduced, and the span can be increased. The hybrid beam developed shows a better performance than the conventional glulam beams.

II. NUMERICAL MODELLING

A. Description of Experiment

In the experiment by Zhang et al. [13], the solid, hollow, and stiffened glulam beam sections were tested. The main parameters studied include the effect of stiffener spacing and the bottom plate's thickness. The bending behaviour was determined by a four-point bending test on glulam beams. This study extended and performed an extensive parametric investigation. Under four-point loading, the effect of aspect ratio on stiffened hollow glulam beam, pattens of different stiffener arrangement and the inclination angle of optimum pattern obtained are studied in detail.

B. Material and Geometrical Modelling

The model of the stiffened glulam beam was developed with the help of ANSYS Workbench. The geometry and experimental data of the work done by Zhang, Xiaofeng, et al. [13] were adopted for developing a finite element model. The dimensions of the model are given in Table I. The various dimension of the specimens is marked in fig.1.

International Journal of Engineering Research & Technology (IJERT)
ISSN: 2278-0181
Vol. 11 Issue 08, August-2022

TABLE I. DIMENSIONS OF MODEL

Name	l (mm)	b (mm)	h (mm)	t_1 (mm)	t_2 (mm)	t_3 (mm)	t_4 (mm)	s (mm)
Z_4	2900	100	150	20	30	20	25	150

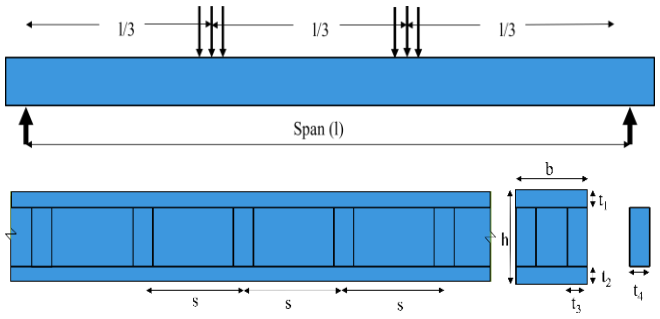

Fig. 1. Hollow glulam beam with the notation [13]

The glulam beam is made of laminated engineered wood products. Thus, it shows anisotropic plastic deformations. Table II shows the material properties of lumber, and Table III shows the mechanical properties of glulam. Fig 3 shows the general stress-strain relation for glulam with f_{wtu} and f_{wcw} are tensile strength and compressive strength parallel to the grain. m refers to the slope of the descending branch, taken as -0.1, E_w is the modulus of elasticity parallel to the grain. ε_{wcu} and ε_{wtu} are the ultimate compressive strain and the ultimate tensile strain, ε_{wcy} is the yield compressive strain. The Hill yield criterion was considered for assigning anisotropic material property to the model. In ANSYS, the elastic material properties are incorporated as engineering constants and non-linear bilinear kinematic hardening with six yield stress ratios. Fig 4 shows the bilinear stress-strain curve adopted for the model.

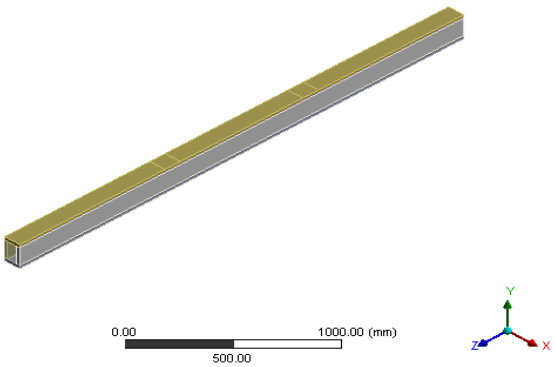

Fig. 2. Glulam beam modelled in ANSYS

TABLE II. MATERIAL PROPERTY OF LUMBER

Category	Average value
Compressive strength parallel to grain (MPa)	55.5
Ultimate compression strain parallel to grain (με)	5073
Bending elastic modulus (MPa)	14016.3

TABLE III. MECHANICAL PROPERTY OF GLULAM

Elastic modulus (MPa)	E_1	14100
	E_2	705
	E_3	705
Shear modulus (MPa)	G_1	1055
	G_2	1055
	G_3	253
Poisson's ratio	υ_1, υ_2	0.3
	υ_3	0.49
Yield stress (MPa)	σ_1	55.5
	σ_1, σ_3	5.5

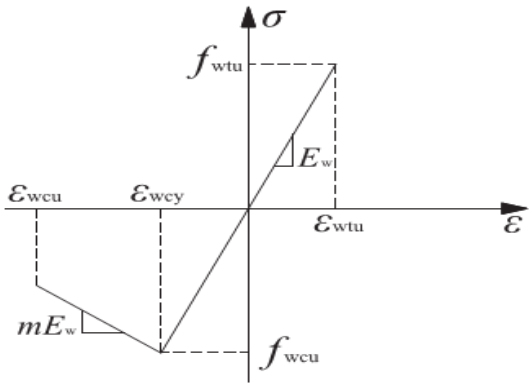

Fig. 3. Generalised stress train curve for glulam

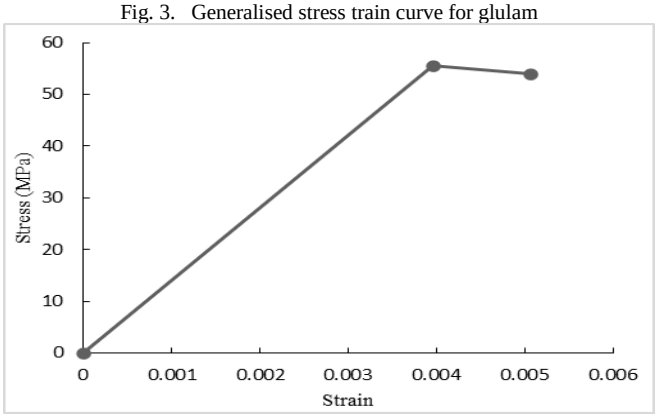

Fig. 4. Bilinear stress-strain curve for the model

C. *Meshing*

A mesh convergence study was conducted, and a mesh size of 12 mm was fixed (program-controlled in ANSYS) for further studies to run the simulations within a reasonable time without compromising accuracy. Hex-dominated structure of Solid 186 meshing is adopted. Fig 5 shows the meshed model in ANSYS software.

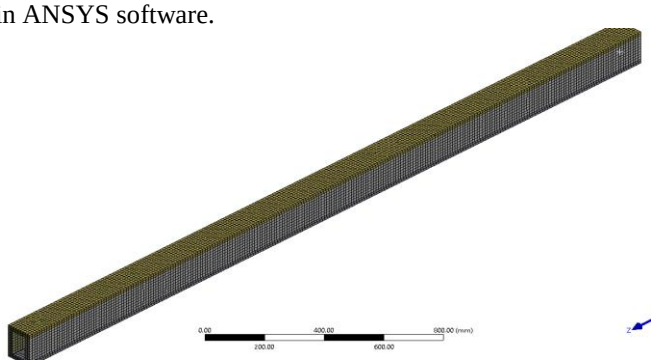

Fig. 5. Meshed model

D. *Loading and Boundary Condition*

The ends of the beam were taken as pinned. As in the experimental setup, pressure load was applied at the top of the beam. The details of various boundary conditions applied to the model are given in Table IV. Fig 6 shows the model with boundary conditions and loading pattern.

International Journal of Engineering Research & Technology (IJERT)
ISSN: 2278-0181
Vol. 11 Issue 08, August-2022

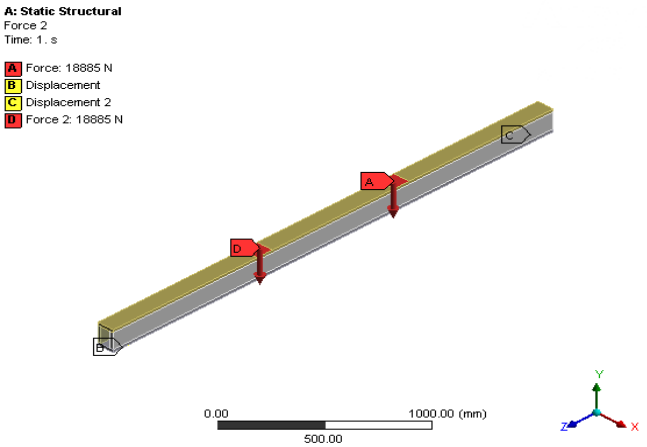

Fig. 6. Boundary conditions applied to the model

TABLE IV. BOUNDARY CONDITIONS

SUPPORT ENDS	U_1	U_2	U_3	UR_1	UR_2	UR_3
Right	0	0	0	1	1	1
left	0	0	1	1	1	1

1-free, 0-arrested

E. Validation

The stress distribution after analysis is shown in fig 7. The load-deflection curve obtained is compared with the experimental results in Fig 9. Experimental specimens and the numerical model by Zhang, Xiaofeng, et al. were used to validate the model. A good agreement between the experimental and numerical model as in fig 8. Since the damage modelling is not considered in the model, some variation in the experimental data is seen. Also, the model behaves like a perfectly plastic model after a certain point.

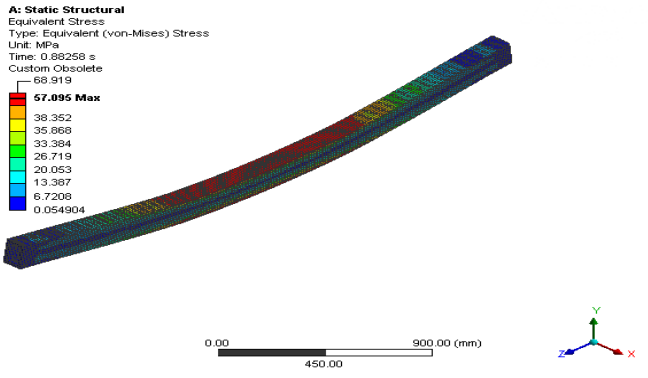

Fig. 7. Stress distribution after analysis

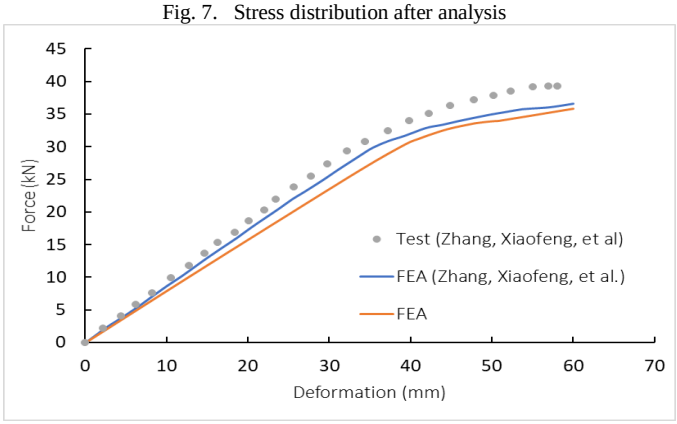

Fig. 8. Load deformation curve for the validated model(Z_4)

III. PARAMETRIC STUDY

A detailed parametric study was conducted on the validated model. About 25 FE models were developed for the study. The first parameter was the effect of aspect ratio on the flexural behaviour of a stiffened hollow glulam beam. Under four-point loading the aspect ratio is varied with constant depth, constant width and the aspect ratio was kept constant, and the dimension is varied. Second parameter considered was the pattern of stiffeners inside the hollow glulam beam and its load carrying capacity. Then an optimum pattern of stiffener arrangement was obtained. For that optimum pattern, the inclination angle is changed, and the bending behaviour is studied.

A. Effect of aspect ratios of beam with constant width

The width of the beam is kept constant as in the validated model. However, the depth is varied, and the behaviour of the beam under four-point loading is studied. The depth of the beam varied from 100 mm to 250 mm. thus the aspect ratio obtained between 0.4 to 1.0. Aspect ratio (AR) is the ratio of the overall width of the beam to its overall depth (b/h). The effect of the aspect ratio in load-carrying capacity is shown fig. 9.

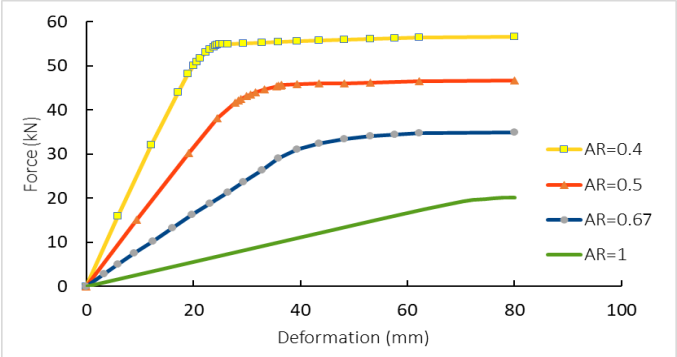

Fig. 9. Load-carrying capacity for varying beam aspect ratio at a constant width.

From the load versus deformation curve, the stiffness of the beam decreases with an increase in aspect ratio. That is, as the depth increases, the stiffness of the beam increases. 180.72% increase in the load-carrying capacity is seen when the aspect ratio decreases from 1.0 to 0.4. However, the percentage change in the peak load has a rate of increase of 73.04%, 57.93%, and 49.75%, respectively. So, a section with an aspect ratio of 0.67 to 0.5 gives considerable stiffness with a higher load-carrying capacity. Percentage change is shown in table V.

TABLE V. PERCENTAGE CHANGE IN ULTIMATE LOAD OBTAINED FOR DIFFERENT ASPECT RATIOS IN CONSTANT WIDTH.

Aspect Ratio	Ultimate load obtained (kN)	Percentage change (%)
1.00	20.18	
0.67	34.92	73.04
0.50	46.61	130.97
0.40	56.65	180.72

B. Effect of aspect ratios of beam with constant depth

The depth of the beam is kept constant as in the validated model. The width is varied, and the behaviour of the beam under four-point loading is studied. The width varied from 100 mm to 250 mm. That is, aspect ratio varies from 0.60 to 1.5, and the corresponding results are shown the fig. 10.

International Journal of Engineering Research & Technology (IJERT)
ISSN: 2278-0181
Vol. 11 Issue 08, August-2022

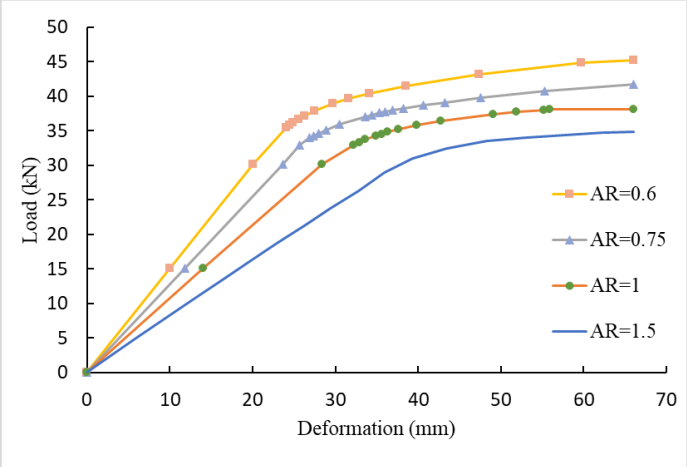

Fig. 10. Load-carrying capacity for varying beam aspect ratio at a constant depth.

The load versus deformation curve shows that, with an increase in aspect ratio, the stiffness of the beam decreased. 32% increase in the load-carrying capacity is seen when the aspect ratio decreased from 1.5 to 0.60. Percentage change is shown in table VI. From the stress distribution, a compressive effect of stiffeners to top and bottom plates are seen as the width increases. So, the bottom and top plate thickness should be increased to avoid localised failure due to the compression of stiffeners to top and bottom plates. The peak load obtained is increased because the loading area is also increased.

TABLE VI. PERCENTAGE CHANGE IN ULTIMATE LOAD OBTAINED FOR DIFFERENT ASPECT RATIOS IN CONSTANT DEPTH.

Aspect Ratio	Ultimate load obtained (kN)	Percentage change (%)
1.50	34.92	
1.00	38.10	9.11
0.75	41.75	19.56
0.60	76.09	31.99

C. *Effect of constant aspect ratios of beam with different dimensions*

The effect of load-carrying capacity is studied by keeping the aspect ratio as a constant. For that, square sections of 100 mm × 100 mm to 250 mm × 250 mm are taken and the aspect ratio is 1.00. The models are named 100, 150, 200, and 250. The effect of the constant aspect ratio is shown the fig. 11.

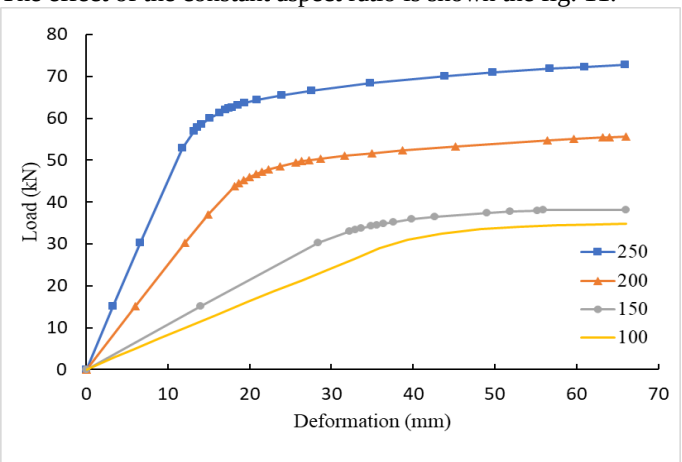

Fig. 11. Load-carrying capacity for a constant beam aspect ratio.

The curve shows that with an increase in dimensions of the model, the stiffness of the beam also increased. A 85.91% increase in the load-carrying capacity is seen when the section dimensions increased from 100 mm to 250 mm. Percentage change in ultimate load is shown in table VII. For 100 mm and 150 mm sections, slightly increased load-carrying capacity is seen. However, beyond 150 mm sections, a significant variation in the load-carrying capacity is seen. From the stress distribution, a slight change is seen, and is due to the localised compressive effect of stiffeners in the beam.

TABLE VII. PERCENTAGE CHANGE IN ULTIMATE LOAD OBTAINED FOR CONSTANT ASPECT RATIO

Model Name	Ultimate load obtained (kN)	Percentage change (%)
100	34.92	
150	38.10	9.11
200	55.61	55.06
250	72.76	85.91

D. *Effect of different patterns of stiffener inclination*

Different patterns of stiffener arrangement in an inclined manner are adopted in this study. The inclination angle of all patterns adopted is 45° and the spacing adopted is uniform if the pattern has space between the stiffeners. The different pattern adopted for the study is demonstrated in fig. 12(a) to fig. 12(f). The load versus deformation curve for each pattern is shown in fig. 13.

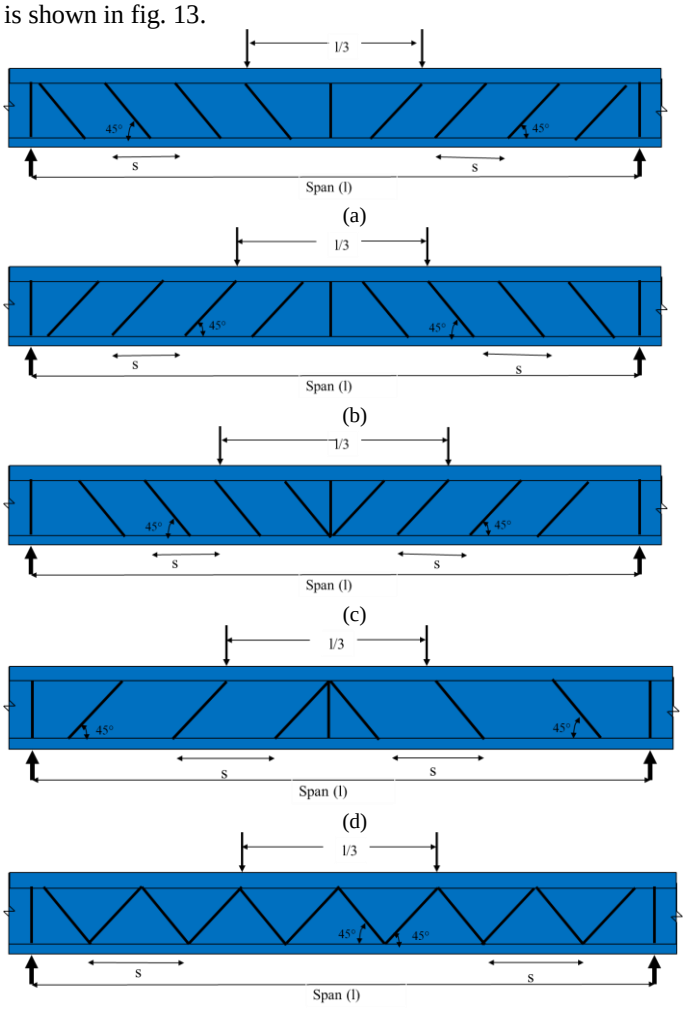

International Journal of Engineering Research & Technology (IJERT)
ISSN: 2278-0181
Vol. 11 Issue 08, August-2022

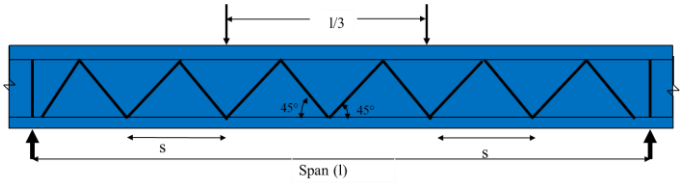

(f)

Fig. 12. Schematic diagram of different patterns of stiffener arrangement adopted.

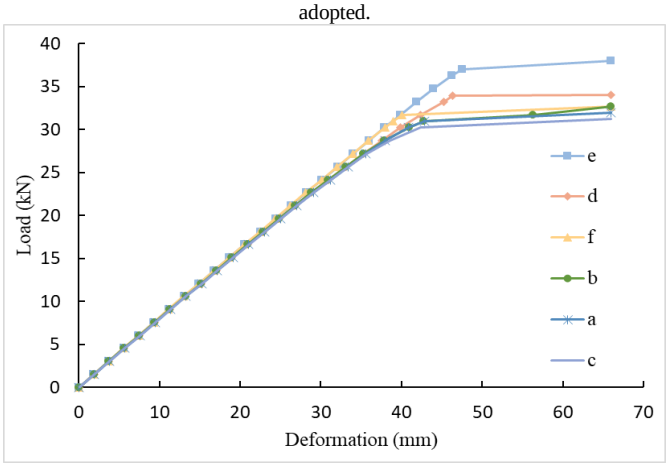

Fig. 13. Load-carrying capacity for different patterns of stiffener arrangement.

From the load-deformation curve, pattern 'e' has a much higher load-carrying capacity than any other stiffener pattern. Thus, the load-deformation curve obtained for the inclined pattern is compared with the vertically stiffened hollow glulam beam, hollow glulam beam, and solid glulam beam. From fig. 13 and fig. 14, it is seen that the inclined stiffened glulam beam (pattern 'e') has a much higher load-carrying capacity than the vertically stiffened glulam beam. The percentage change obtained for each stiffener pattern with respect to solid, hollow, stiffened hollow glulam beams are shown in table VIII.

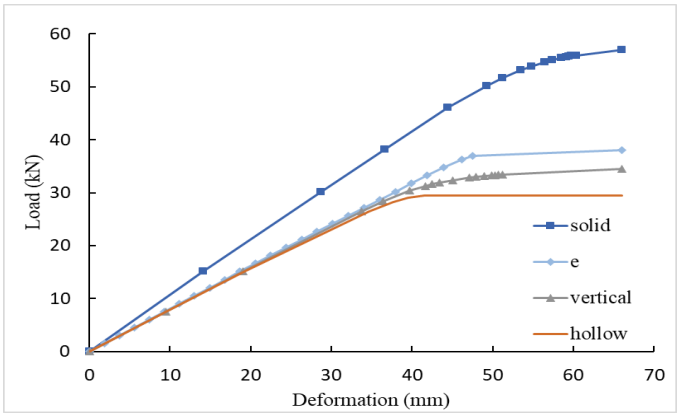

Fig. 14. Comparison of the load-carrying capacity of beams with and without stiffeners.

TABLE VIII. PERCENTAGE CHANGE IN ULTIMATE LOAD OBTAINED FOR DIFFERENT PATTERNS OF STIFFENER ARRANGEMENT.

Model Name	Ultimate load obtained (kN)	Percentage change with vertically stiffened beam (%)	Percentage change with hollow glulam beam (%)	Percentage change with solid glulam beam (%)
a	31.97	-7.78	8.22	-78.17
b	32.73	-5.28	10.80	-74.04
c	31.21	-10.40	5.66	-82.50
d	34.09	-1.09	15.39	-67.11
e	38.01	10.31	28.68	-49.86
f	32.73	-5.30	10.78	-74.07

E. Effect of different angles of inclinations

From the parametric study conducted on different patterns of stiffeners, fig. 14 shows an optimum higher value of load-carrying capacity than the vertically arranged stiffener pattern. Thus, the inclination angle is changed. Also, the stiffener is arranged so that the stiffener's ends should be at the loading point, and a vertical stiffener is provided at the support condition. The angles adopted are within the range of 0° to 45°. The thickness of the different members in the beam is kept constant. This study has some limitations; the stiffeners should end at the loading points. Thus, the angle adopted is 17°, 32°, and 45° with the bottom plate. Thus the models are denoted as 1v, 2v, and 3v respectively. Solid, hollow, and vertically stiffened glulam beams are also considered for better understanding. The result obtained after the analysis is shown in fig. 15. From the curve, the 2v model (with an angle of 32°) shows a much higher value of load-carrying capacity.

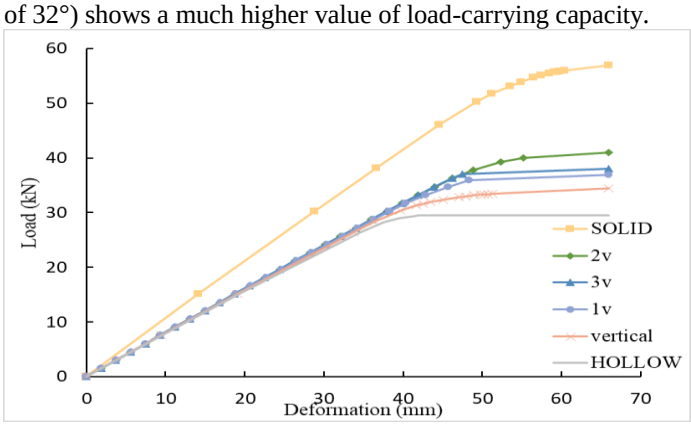

Fig. 15. Load-carrying capacity for inclined stiffened glulam beams with different angles.

TABLE IX. PERCENTAGE CHANGE IN ULTIMATE LOAD OBTAINED FOR DIFFERENT INCLINATION ANGLES.

Model Name	Ultimate load obtained (kN)	Percentage change with vertically stiffened beam (%)	Percentage change with hollow glulam beam (%)	Percentage change with solid glulam beam (%)
1v	36.88	7.03	24.85	-54.45
2v	41.03	19.08	38.90	-38.83
3v	38.01	10.31	26.68	-49.86

IV. CONCLUSIONS

Various studies on the bending behaviour of glulam beam under four-point loading observed that aspect ratio with constant depth has a significance than aspect ratio with constant depth. Also, the inclined stiffener pattern has a higher load carrying capacity with an inclination angle of 32° Therefore, this study investigates the effects of various beam aspect ratio in the stiffened hollow glulam beam. From the parametric study, the following conclusions are arrived at:

i. With a decrease in beam aspect ratio, the load carrying capacity is increased. As the aspect ratio decreases from 1.0 to 0.40 with a constant with, the load-carrying capacity is increased by 180.72%. Whereas, for a constant depth the variation is only 32%.

International Journal of Engineering Research & Technology (IJERT)
ISSN: 2278-0181
Vol. 11 Issue 08, August-2022

ii. For a constant aspect ratio, with increase in dimensions leads to increased load carrying capacity. A section dimension greater than 150 mm × 150 mm shows a significant increase in load carrying capacity.

iii. A zig-zag pattern of stiffener arrangement shows a higher load carrying capacity than the vertically stiffened hollow glulam beam. The optimum pattern obtained has an inverted v shape at the loading point.

iv. For the inclined stiffener pattern, the inclination is varied between 0° and 45°. An angle with 32° with 2v shape in between the loading points shows a higher load carrying capacity.

REFERENCES

[1] A handbook of glulam., Holger Gross, Gross Produktion AB, Stockhol, Sweden, 3rd edition, Vol. 1, 2013.

[2] ANSI:117-2010: Standard specification for structural glued laminated timber of softwood species, ANSI, 2010.

[3] ASTM D198-2015, Static flexural tests of lumber in structural sizes, ASTM, 2015.

[4] Buchanan, A. H. (1990). Bending strength of lumber. *Journal of structural engineering*, *116*(5), 1213-1229. https://doi.org/10.1061/(ASCE)0733-9445(1990)116:5(1213)

[5] Du, H., Hu, X., Xie, Z., & Meng, Y. (2021). Experimental and analytical investigation on fire resistance of glulam-concrete composite beams. *Journal of Building Engineering*, *44*, 103244. https://doi.org/10.1016/j.jobe.2021.103244

[6] Ferrier, E., P. Labossière, and K. W. Neale. (2012) Modelling the bending behaviour of a new hybrid glulam beam reinforced with FRP and ultra-high-performance concrete. *Applied Mathematical Modelling* 36.8. https://doi.org/10.1016/j.conbuildmat.2015.07.116

[7] Fossetti, M., Minafò, G., & Papia, M. (2015). Flexural behaviour of glulam timber beams reinforced with FRP cords. *Construction and Building Materials*, *95*, 54-64.

[8] Issa, C. A., & Kmeid, Z. (2005). Advanced wood engineering: glulam beams. *Construction and Building Materials*, *19*(2), 99-106. https://doi.org/10.1016/j.conbuildmat.2004.05.013

[9] Sun, X., He, M., & Li, Z. (2020). Novel engineered wood and bamboo composites for structural applications: State-of-art of manufacturing technology and mechanical performance evaluation. *Construction and Building Materials*, *249*, 11875. https://doi.org/10.1016/j.conbuildmat.2020.118751

[10] Timbolmas, C., Bravo, R., Rescalvo, F. J., & Gallego, A. (2022). Development of an analytical model to predict the bending behavior of composite glulam beams in tension and compression. *Journal of Building Engineering*, *45*, 103471. https://doi.org/10.1016/j.jobe.2021.103471

[11] Vida, C., Lukacevic, M., Eberhardsteiner, J., & Füssl, J. (2022). Modeling approach to estimate the bending strength and failure mechanisms of glued laminated timber beams. *Engineering Structures*, *255*, 113862. https://doi.org/10.1016/j.engstruct.2022.113862

[12] Wang, Y., Hou, Q., Xu, T., Qu, S., & Zhang, B. (2021). The bending-shear behaviors of steel reinforced fast-growing poplar glulam beams with different shear-span ratios. *Construction and Building Materials*, *300*, 124008. https://doi.org/10.1016/j.conbuildmat.2021.124008

[13] Zhang, X., Luo, J., Luo, L., Sun, Y., & Li, Z. (2022). Experimental and numerical investigation into the bending behaviour of stiffened hollow glulam beams. *Journal of Building Engineering*, *45*, 103488..